Protocol for generating multiphoton entangled states from quantum dots in the presence of nuclear spin fluctuations

Emil V. Denning,[1,*] Jake Iles-Smith,[1] Dara P. S. McCutcheon,[2] and Jesper Mork[1,†]

[1]*Department of Photonics Engineering, DTU Fotonik, Technical University of Denmark, Building 343, 2800 Kongens Lyngby, Denmark*

[2]*Quantum Engineering Technology Labs, H. H. Wills Physics Laboratory and Department of Electrical and Electronic Engineering, University of Bristol, Bristol BS8 1FD, United Kingdom*

Multiphoton entangled states are a crucial resource for many applications in quantum information science. Semiconductor quantum dots offer a promising route to generate such states by mediating photon-photon correlations via a confined electron spin, but dephasing caused by the host nuclear spin environment typically limits coherence (and hence entanglement) between photons to the spin T_2^* time of a few nanoseconds. We propose a protocol for the deterministic generation of multiphoton entangled states that is inherently robust against the dominating slow nuclear spin environment fluctuations, meaning that coherence and entanglement is instead limited only by the much longer spin T_2 time of microseconds. Unlike previous protocols, the present scheme allows for the generation of very low error probability polarization encoded three-photon GHZ states and larger entangled states, without the need for spin echo or nuclear spin calming techniques.

I. INTRODUCTION

A crucial requirement for photonic measurement-based quantum computing schemes is a resource of entangled states [1–10]. The generation of such states is being pursued on various platforms; among these are continuous variable quantum optics [11], spontaneous parametric down-conversion in nonlinear crystals [12], nitrogen-vacancy centers [13], and self-assembled semiconductor quantum dots (QDs) [14]. QDs in particular are attractive due to the combination of their excellent optical properties [15–19], and the prospect of deterministic interactions with single photons [15,20]. By charging a QD with a single electron, it becomes equipped with an internal spin degree of freedom that couples to the polarization of optical photons [21], while also benefiting from highly developed optical control and readout techniques [22–30]. Using these properties, it is possible to generate spin-photon entanglement [31,32], and by entangling a sequence of photons with a QD, spin-multiphoton states are generated, reducing to multiphoton entangled states once the QD spin is measured [33–35].

A considerable challenge for the QD platform is posed by the interaction of the QD spin with its nuclear spin environment, which gives rise to a slowly fluctuating magnetic Overhauser field [36,37]. Due to uncertainty in the Overhauser field, phase coherence between the QD spin states is lost on a time scale set by the spread of available Overhauser states, limiting the QD spin coherence to typically only a few nanoseconds [38–40] (usually termed the T_2^*, ensemble, or inhomogeneous dephasing time). This renders practical implementations to generate states beyond spin–single-photon entanglement extremely challenging in their original formulations [31–35,41]. Spin coherence times can in principle be extended beyond T_2^* by applying spin echo or dynamical decoupling sequences which unwind fluctuating phase

evolution [38,42]. However, this not only adds operational complexity, but, in cases which utilize photon frequency degrees of freedom [43], will not extend photon coherence times, as the Overhauser field is imprinted onto the photonic component of the state not affected by echo pulses. Spin coherence may also be extended by polarization of the nuclear environment [39,44–49], though a very high ($>$90%) and as yet unachievable degree of polarization is required.

II. DEPHASING-RESILIENT PROTOCOL

As a solution to this, we propose a QD-based protocol to generate multiphoton entangled states that is naturally robust against slow Overhauser field fluctuations, with the coherence being instead limited only by faster pure-dephasing (homogeneous) processes, with a typical time scale of microseconds (termed the T_2 time). The central feature of our proposed protocol is that it combines (1) an external field to ensure the nuclear environment gives rise to a fluctuating magnetic field amplitude only, with (2) narrow-band excitation, which means an entangled state is generated in which all terms have the same energy. This means only a global inconsequential phase is acquired over time, thus ensuring robustness against the dominating slow nuclear spin fluctuations. We benchmark our protocol against a multiphoton extension of the experimental realizations in Refs. [43,50,51] and the theoretical schemes in Refs. [31,33], showing that with realistic noise models these cannot be scaled to create entanglement beyond the spin–single-photon regime as they lack one or both of the above properties. Using the proposed protocol in combination with a suitable frequency quantum eraser, we show that three-photon GHZ states can be generated near deterministically with near-unity fidelity, and without any active measures taken to avoid nuclear spin dephasing. Several of these microclusters could then be efficiently transformed to a large cluster state using only passive linear optical elements [52].

Our protocol is based on a negatively charged QD in a single-sided, polarization-degenerate cavity, operating in the weak-coupling regime. An external magnetic field

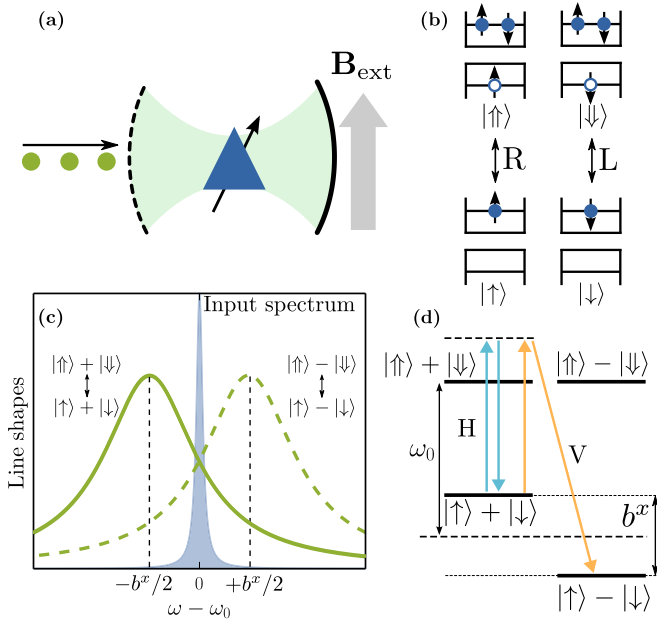*emil.denning@gmail.com
†jesm@fotonik.dtu.dk

FIG. 1. (a) QD in a polarization-degenerate, single-sided cavity is exposed to an external magnetic field perpendicular to the cavity axis. (b) Electron and hole configurations for the ground states and trions, which in zero field are connected via circularly polarized transitions. (c), (d) The Voigt-geometry magnetic field leads to linearly polarized transitions (labeled H and V) between hybridized levels as indicated, split by the Zeeman energy b^x. Shown in (c) is a spectrally narrow photon resonant with the zero field transition energy ω_0, which can lead to a spin-flip Raman scattering process changing the photon's energy and polarization [orange arrows in (d)], or a coherent scattering process leaving energy and polarization unchanged (blue arrows). Occurring in superposition these processes lead to spin-photon entanglement.

perpendicular to the optical axis splits the QD transitions, and results in linearly polarized transitions to the excited trion states. We now consider an H-polarized photon incident on the cavity, with the QD in the external magnetic-field eigenstate $|\phi_+\rangle = (1/\sqrt{2})(|\uparrow\rangle + |\downarrow\rangle)$, where $|\uparrow\rangle$ and $|\downarrow\rangle$ denote the ground-state electron spin projection along the optical axis (defining the z direction). If the incoming photon is resonant with the bare QD transition energy in zero field, labeled ω_0, there are two off-resonant scattering possibilities. A Raman transition can take place, in which the spin of the QD is flipped, and the photon frequency and polarization are changed [orange arrows in Fig. 1(d)], or the photon can coherently scatter, leaving it and the QD unchanged (blue arrows). As such, the composite QD-photon system will evolve in superposition, and we write a single-photon scattering event as $|H,\omega_0\rangle_1|\phi_+\rangle \rightarrow |\psi^{(1)}\rangle$ with

$$|\psi^{(1)}\rangle \equiv \frac{1}{\sqrt{2}}(|H,\omega_0\rangle_1|\phi_+\rangle - i|V,\omega_+\rangle_1|\phi_-\rangle), \quad (1)$$

where $\omega_\pm = \omega_0 \pm (b^x/2)$ with b^x being the Zeeman splitting, and $|\alpha,\omega\rangle_i$ denoting photon i in polarization state α with frequency ω. The superscript on $|\psi^{(n)}\rangle$ denotes the photon number in the scattered state.

A second photon can then be sent to the QD-cavity system after some time, and the total composite state will be the three-

qubit entangled state (cf. Appendix C for details):

$$\begin{aligned}|\psi^{(2)}\rangle = \tfrac{1}{2}(|H,\omega_0\rangle_1\{|H,\omega_0\rangle_2|\phi_+\rangle - i|V,\omega_+\rangle_2|\phi_-\rangle\} \\ + |V,\omega_+\rangle_1\{-i|H,\omega_0\rangle_2|\phi_-\rangle + |V,\omega_-\rangle_2|\phi_+\rangle\}). \quad (2)\end{aligned}$$

This state is local unitary equivalent (LUE) to a three-qubit linear cluster state [8] and a GHZ state, provided that the frequency degree of freedom is erased. For three or more photons, the state is no longer LUE to a GHZ or linear cluster state, though it possesses a rich entanglement structure with maximal localizable entanglement and infinite entanglement length. Of particular note, when the QD spin is projected out of the state $|\psi^{(3)}\rangle$ in the $\{\phi_\pm\}$ basis, the remaining state is LUE to a three-photon polarization encoded GHZ state [53].

The most important feature of Eq. (2), however, is that each term has the same total energy. This is because the first Raman process flips the spin from $|\phi_+\rangle$ to $|\phi_-\rangle$, transferring energy b^x from the QD to the photon. In the second spin-flip event, the opposite happens, and the photon transfers energy b^x to the QD. Consequently, the state $|\psi^{(n)}\rangle$ for any n consists of a large superposition of trajectories that all share the same total energy $n\omega_0 + b^x/2$, and $|\psi^{(n)}\rangle$ will acquire only a global phase in time. Crucially, this means that when an ensemble of states such as $|\psi^{(n)}\rangle$ is prepared, phase coherence between terms in the superposition is protected from any fluctuations in b^x that may occur between one realization and another. In particular, for a single QD, slow variations in the Overhauser field over time will not decohere $|\psi^{(n)}\rangle$, allowing, for example, the generation of three-photon GHZ states with near-unit fidelity.

As this insensitivity to nuclear spin interactions is the essential feature of our protocol, we now consider it in more detail. The dominant coupling between the QD electron spin and nuclear spins is the hyperfine interaction [54]. If this is much weaker than the electron Zeeman energy and the number of nuclear spins is large, its effect can be modeled as a magnetic Overhauser field, $\mathbf{B}_N$ [37], which can be added to the external field to give $\mathbf{B} = \mathbf{B}_{\text{ext}} + \mathbf{B}_N$. Due to the large number of nuclear spins $\mathbf{B}_N$ evolves on a slow microsecond time scale, as compared to the characteristic nanosecond time scale governing the electron spin dynamics [37]. This allows us to model the Overhauser field as being stationary during a single experimental run, but probabilistically chosen from $w(B_N^i; \Delta_B) = 1/(\Delta_B\sqrt{2\pi}) \exp[-(B_N^i)^2/(2\Delta_B^2)]$, describing a Gaussian distribution with zero mean for each of the Cartesian components, B_N^i, and with standard deviation Δ_B [37]. If the external field $\mathbf{B}_{\text{ext}} = B_{\text{ext}}\hat{\mathbf{x}}$ is appreciably stronger than Δ_B, we can assume that the components of $\mathbf{B}_N$ parallel to $\mathbf{B}_{\text{ext}}$ dominate [37]. In such a case nuclear spins can be included by writing the effective Zeeman splitting as $b^x = g_e\mu_B(B_{\text{ext}} + B_N^x)$, with g_e the electron Landé factor and μ_B the Bohr magneton, and with B_N^x averaged over using $w(B_N^x; \Delta_B)$.

To see how ensemble dephasing can arise, consider a simple superposition state in the magnetic-field eigenstate basis $(1/\sqrt{2})(|\phi_+\rangle + |\phi_-\rangle)$. For times t less than a microsecond, this state becomes $|\varphi\rangle = (1/\sqrt{2})(e^{-ib^xt/2}|\phi_+\rangle + e^{ib^xt/2}|\phi_-\rangle)$ in a single realization. An ensemble of such states, however, samples all Overhauser fields, giving the single-spin density operator $\varrho = \int dB_N^x w(B_N^x; \Delta_B)|\varphi\rangle\langle\varphi|$, and we find that coherences decay as $\langle\phi_+|\varrho|\phi_-\rangle \propto \exp[-(t/T_2^*)^2]$ with $T_2^* = \sqrt{2}/(g_e\mu_B\Delta_B)$, which for typical InGaAs QDs corresponds

to nanoseconds. Crucially, however, in our protocol, states such as $|\varphi\rangle$ above are never produced. Instead, assuming that all scattering processes take place within the microsecond time scale over which the Overhauser field can be considered constant, after accumulating n photons in the composite state, it will have the form $|\psi^{(n)}\rangle = (|\psi_+^{(n)}\rangle|\phi_+\rangle + |\psi_-^{(n)}\rangle|\phi_-\rangle)/\sqrt{2}$, as we show in Appendix C. Here $|\psi_\pm^{(n)}\rangle$ is an entangled n-photon state, in which all terms have energy $\Omega_+ = n\omega_0$ or $\Omega_- = n\omega_0 + b^x$. This form eliminates the inhomogeneous ensemble dephasing as described above, as the phase can be factored out of the complete state. Dephasing only occurs on a much longer time scale of the T_2 time set by pure-dephasing processes, and typically corresponding to microseconds [37]. If the spin is measured in the basis $\{\phi_+, \phi_-\}$ while the Overhauser field is unchanged, the photonic state is projected to one of the states $|\psi_\pm^{(n)}\rangle$, which are also robust against ensemble dephasing. Though we have emphasized resilience to Overhauser field fluctuations, by the same arguments our scheme is also robust against any other slow processes leading to energy-level fluctuations, most notably those caused by charge noise [40,55].

Having shown that our protocol is robust against ensemble dephasing processes, we now turn our attention to another potential imperfection, that arising from the photon scattering process itself, which we term the *scattering fidelity*. We are interested here in a quantitative analysis of how well the entangled states in Eqs. (1) and (2) are produced given a realistic QD-cavity model. To assess this, we write the total Hamiltonian as $\hat{H} = H_0(t) + H_B$, where $H_0(t)$ is the QD-cavity Hamiltonian including light-matter interactions, and H_B contains the magnetic field. In a frame rotating at ω_0 we have (we set $\hbar = 1$) $H_0(t) = \eta(t)\mathbf{e}_{\text{in}}^\dagger \mathbf{A} + g\Sigma^\dagger \mathbf{A} + \text{H.c.}$, with $\mathbf{A} = (a_+, a_-)^{\text{T}}$ the polarization-resolved vectorial cavity mode operator in the circular polarization basis, $\Sigma = (|\uparrow\rangle\langle\Uparrow|, |\downarrow\rangle\langle\Downarrow|)^{\text{T}}$, and g is the QD-cavity coupling strength. The incoming light is modeled as a weak coherent pulse, described by a time-dependent driving of the cavity field, taken to be Gaussian, $\eta(t) = \eta_0 \exp[-(t/t_0)^2]$, and $\mathbf{e}_{\text{in}}$ is the input polarization Jones vector in the circular basis. The magnetic-field Hamiltonian is $H_B = \mu_B \mathbf{B} \cdot (g_e \mathbf{S}_e - g_h \mathbf{S}_h)$, with $\mathbf{S}_e$ ($\mathbf{S}_h$) the vectorial spin operator for the electron (hole) subspace and g_h the hole Landé factor [56]. With a numerical solution of the dynamics generated by the Hamiltonian [57], the scattering fidelity for an n photon state is simply $\mathcal{F}^{(n)} = \text{Tr}[\rho|\tilde{\psi}^{(n)}\rangle\langle\tilde{\psi}^{(n)}|]$, where ρ is the numerically calculated QD-photon density operator and $|\tilde{\psi}^{(n)}\rangle\langle\tilde{\psi}^{(n)}|$ the ideal maximally entangled state [58]. Additional details about the dynamical model and calculation of fidelities can be found in Appendixes A and B.

By first artificially setting the Overhauser field to zero, in Fig. 2(a) we show how the spin-one photon Bell state fidelity $\mathcal{F}^{(1)}$ can be optimized by tuning the external magnetic field. We see that near-unity scattering fidelity is reached when the external field is approximately the cavity-enhanced QD linewidth, $b_{\text{ext}} \simeq \Gamma_{\text{cav}} = 4g^2/\kappa$, as it is depicted in Fig. 1(c). This ensures that an incoming photon has a high probability of scattering off one of the two possible transitions while also ensuring that they are adequately separated. In this regime, the fidelity is limited by the finite bandwidth of the input photon, since any off-center frequency components lead to
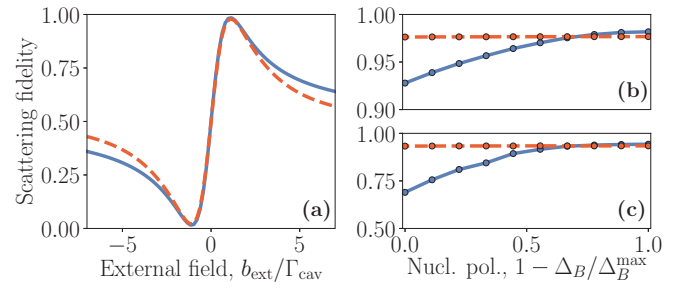

FIG. 2. (a) One photon scattering fidelity $\mathcal{F}^{(1)}$ with respect to the ideal Bell state, $(1/\sqrt{2})(|x\rangle|\phi_+\rangle - i|y\rangle|\phi_-\rangle)$, as function of external magnetic field in the absence of Overhauser field fluctuations. Blue solid lines correspond to a low Q-factor cavity ($\kappa = 10^3$ ns^{-1}, $Q \simeq 2000$); red dashed lines represent a high Q-factor cavity ($\kappa = 150$ ns^{-1}, $Q \simeq 13000$). Other parameters: $t_0 = 8/\Gamma_{\text{cav}}$, $g = 15$ ns^{-1}, $g_h/g_e = 0.2$, $\eta_0/\kappa = 10^{-3}$ (10^{-2}) for the low (high) Q cavity and $g_e\mu_B\Delta_B^{\text{max}} = 0.2$ ns^{-1}. (b) Fidelity $\mathcal{F}^{(1)}$ including nuclear spin noise as a function of the degree of nuclear spin polarization. The external field has been tuned to the optimal value found numerically in (a). Line styles represent parameters as in (a). Circles and error bars indicate ensemble averages and (25%, 75%) quantiles of the fidelity. (c) Fidelity $\mathcal{F}^{(2)}$ with respect to the ideal spin–two-photon state, obtained by scattering two photons on the QD with a time delay of $3t_0$.

an unevenly weighted superposition in the scattered state. In Figs. 2(b) and 2(c), we show the fidelities $\mathcal{F}^{(1)}$ and $\mathcal{F}^{(2)}$ including the nuclear environment, shown as a function of the nuclear environment polarization, ranging from maximally unpolarized ($\Delta_B = \Delta_B^{\text{max}}$) to the fully polarized ($\Delta_B = 0$) regime, and for high (red, dashed curve) and low (blue, solid) cavity Q factors, corresponding to QDs with broad and narrow Purcell-enhanced transition lines. We see that even for an unpolarized nuclear environment, fidelities of the two-photon state are above 90% for $Q = 13\,000$. Higher Q factors are advantageous since they correspond to larger QD linewidths and hence larger optimal external field strengths, which in turn mean the strength of the external field relative to the Overhauser field is greater. This results in increased stability of the QD eigenstructure and purity of the QD-photon scattering process, while also ensuring that the Overhauser field leads only to fluctuations in the magnitude of the field.

We emphasize that the internal photon-QD interaction in the protocol is in principle deterministic, with the quantum efficiency being limited only by scattering of light into non-cavity modes, which is heavily suppressed in moderate to high Q cavities [17,19]. To obtain a purely polarization-entangled state, however, it is necessary to erase the frequency degree of freedom in $|\psi^{(n)}\rangle$. This is an unavoidable consequence of the state's insensitivity to ensemble dephasing, and could be achieved, for example, using fast single-photon detectors [59,60] or ultrafast nonlinear frequency converters [51].

III. COMPARISON TO ALTERNATIVE PROTOCOLS

To benchmark our protocol, we compare it to three alternative existing schemes. The first scheme (Protocol A) is based on coherent scattering of single linearly polarized photons on a charged QD in the absence of an external field [31,32]. Using
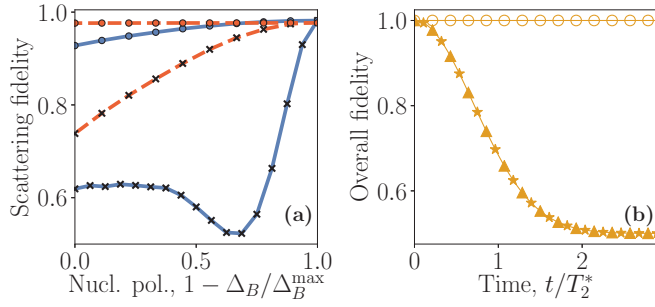
FIG. 3. Comparison of the present scheme with existing Protocols A, B, and C described in the main text. (a) Ensemble-averaged spin–one-photon Bell state scattering fidelity $\mathcal{F}^{(1)}$ as in Fig. 2(b) for protocol A (crosses) and for the present scheme [circles, already shown in Fig. 2(b)]. Red and blue lines correspond to high and low Q-factor parameters as in Fig. 2(b). (b) Ensemble-averaged photonic state fidelity after spin projection as a function of time, assuming unit scattering fidelity, shown for Protocols B (stars) and C (triangles). Both show a rapid decay due to large spread of possible Overhauser fields, while the present scheme (circles) is unaffected due to the form of Eq. (1) which acquires only a global phase in time.

our noise model, we calculate the scattering fidelity of this protocol in the presence of the same realistic nuclear spin environment. The fidelity of generating the spin–one-photon Bell state $\mathcal{F}^{(1)}$ is shown in Fig. 3(a), where crosses indicate values using Protocol A, and the circles correspond to values using the present dephasing-resilient scheme [already shown in Fig. 2(b)]. We see that the scattering fidelity of Protocol A is generally low, reaching values close to unity only for very high degrees of nuclear spin polarization. The reason for this protocol's sensitivity to dephasing processes can be attributed to its lack of an external field, which leaves the QD eigenstructure highly exposed to Overhauser field fluctuations.

The second alternative scheme we consider (Protocol B) is a multiphoton extension of the schemes used in Refs. [43,50,51], that use emission of a QD in an external in-plane field. This protocol resembles the scheme we propose here, but with the crucial difference that single-photon scattering in our scheme is replaced by full π-pulse excitations followed by spontaneous emission. While the magnetic field does ensure stability of the spin eigenstructure and high scattering fidelity (unlike Protocol A), the spectrally broad π pulses mean energy is not conserved in all paths of the evolution. As we show in Appendix D, the result is that the n-photon state contains terms which acquire phases that depend on the fluctuating total effective Zeeman energy $b^x = g_e\mu_B(B_{\text{ext}} + B_N^x)$ in different ways, and the state therefore loses its phase coherence on a short $T_2^* = \sqrt{2}/(g_e\mu_B\Delta_B) \sim$ ns time scale, in much the same way as a single electron spin. Fidelities of a two-photon state obtained after excitation with two π pulses followed by spin projection are shown in Fig. 3(b) with stars, where unit scattering fidelity is assumed, and t represents time after spin projection. Also shown with triangles is the corresponding two-photon state fidelity for the linear cluster state generation proposal of Ref. [33], Protocol C, again assuming unit scattering fidelity. As in the case of Protocol B, this scheme is also sensitive to ensemble dephasing of the electron spin. The form of Eq. (1), however, ensures the present scheme does not dephase

by this mechanism, leading to coherence times well beyond nanoseconds, as shown by the open circles.

In summary, we have presented a spin-mediated multiphoton entanglement protocol which is robust against slow Overhauser field fluctuations, meaning that coherence is limited to the pure spin dephasing time T_2 of microseconds, rather than the inhomogeneous dephasing time T_2^* of nanoseconds. With a suitable frequency eraser, the protocol can be used as a source of high-fidelity three-photon GHZ states, which through linear optical operations can be transformed to a universal quantum resource for measurement-based quantum computing [52]. We emphasize that no spin echo or nuclear polarization techniques are necessary, and that optical excitation could be achieved with readily obtainable weak coherent laser pulses, or instead with narrow-band single photons for deterministic operation.

APPENDIX A: DESCRIPTION OF MODEL

We consider a singly negatively charged quantum dot (QD) in a one-sided cavity, which is driven by a polarized weak optical pulse. The cavity field is resolved in two orthogonal circular polarizations with mode operators a_+ and a_-, satisfying $[a_\lambda, a_{\lambda'}^\dagger] = \delta_{\lambda\lambda'}$, $[a_\lambda, a_{\lambda'}] = [a_\lambda^\dagger, a_{\lambda'}^\dagger] = 0$. We assume that the cavity is resonant with the QD transition at a frequency of ω_0. Further, the cavity is coupled to the optical electromagnetic environment, resolved in two polarizations with mode operators $b_{\lambda q}$, where $\lambda = \pm$ denotes the polarization and q denotes the mode index. As a basis for the QD, we use the spin eigenstates projected along the z direction, taken as the optical axis. For the charged ground states, these are $|\uparrow\rangle$ and $|\downarrow\rangle$, while for the corresponding trion states they are $|\Uparrow\rangle$ and $|\Downarrow\rangle$, denoting the heavy-hole spin states with spin projection eigenvalues $J_z = \pm 3/2$. Due to isotropic strain, the light holes with $J_z = \pm 1/2$ are split off from the heavy holes by an energy, Δ_{LH}, much larger than the linewidth of the transition, and we can ignore them in the light-matter interaction [61]. The QD is subject to a magnetic field, **B** in an arbitrary direction described by the polar (azimuthal) angle, θ (ϕ), and with a magnitude of B. Moving to a frame rotating with the resonance frequency, ω_0, the total Hamiltonian can be written as $\hat{H}(t) = H_0(t) + H_B + H_{\text{EM}}^0 + H_{\text{EM}}^I$, with ($\hbar = 1$)

$$H_0(t) = \eta(t)\mathbf{e}_{\text{in}}^\dagger \mathbf{A} + g\Sigma^\dagger \mathbf{A} + \text{H.c.},$$

$$H_B = \mu_B \mathbf{B} \cdot (g_e \mathbf{S}_e - g_h \mathbf{S}_h),$$

$$H_{\text{EM}}^0 = \sum_{\lambda q}(\omega_q - \omega_0)b_{\lambda q}^\dagger b_{\lambda q},$$

$$H_{\text{EM}}^I = \sum_{\lambda q} g_q b_{\lambda q} a_\lambda^\dagger + \text{H.c.}, \tag{A1}$$

where $\mathbf{A}$ is the polarization-resolved vectorial mode operator $(a_+, a_-)^{\mathrm{T}}$, $\Sigma = (|\uparrow\rangle\langle\Uparrow|, |\downarrow\rangle\langle\Downarrow|)^{\mathrm{T}}$ is the spin-resolved QD transition operator, g is the QD-cavity coupling rate, μ_B is the Bohr magneton, g_e (g_h) is the electron (hole) Landé factor, $\mathbf{S}_e$ ($\mathbf{S}_h$) is the vectorial spin operator for the electron (hole) subspace, ω_q is the frequency of the qth environmental mode, and g_q is the coupling rate between the cavity and the qth environmental mode. The pulse envelope, $\eta(t)$, is taken to be Gaussian, $\eta(t) = \eta_0 \exp[-(t/t_0)^2]$, and $\mathbf{e}_{\mathrm{in}}$ the input polarization Jones vector in the circular basis.

To write down a practical form of H_{B}, we use the spin eigenstates as a basis. For the electron spin in the ground-state manifold, we use the Zeeman eigenstates determined by the direction of the magnetic field, $|\phi_+\rangle = \cos\theta/2|\uparrow\rangle + e^{i\phi}\sin\theta/2|\downarrow\rangle$, $|\phi_-\rangle = e^{-i\phi}\cos\theta/2|\uparrow\rangle - \sin\theta/2|\downarrow\rangle$. As for the trion spin, treating the magnetic-field interaction perturbatively to first order in the parameter $\mu_B g_h B/\Delta_{\mathrm{LH}}$, the light- and heavy-hole manifolds remain uncoupled. The heavy-hole eigenstates are then $|\Downarrow\rangle$ and $|\Uparrow\rangle$ with associated energies $\pm 3/2\mu_B g_h B \cos\theta$. In this basis, H_{B} takes the form

$$H_{\mathrm{B}} = -\frac{3}{2}\tilde{g}_h b \cos\theta(|\Uparrow\rangle\langle\Uparrow| - |\Downarrow\rangle\langle\Downarrow|)$$
$$+ \frac{b}{2}(|\phi_+\rangle\langle\phi_+| - |\phi_-\rangle\langle\phi_-|), \tag{A2}$$

with $b = \mu_B g_e B$ and $\tilde{g}_h = g_h/g_e$.

The interaction with the electromagnetic environment can be simplified by applying a standard Born-Markov approximation, corresponding to assuming a flat spectral density over the relevant frequency range [62]. With this approximation and neglecting the environmentally induced Lamb shift, the perturbative master equation treating H_{EM}^I to second order is $\dot{\rho}(t) = \mathcal{L}(t)\rho(t)$ with $\mathcal{L}(t)$ the time-dependent Liouvillian,

$$\mathcal{L}(t) = -i[H_0(t) + H_{\mathrm{B}}, \cdot] + \kappa\sum_{\lambda=\pm}\left(a_\lambda \cdot a_\lambda - \frac{1}{2}\{a_\lambda^\dagger a_\lambda, \cdot\}\right),$$
$$\tag{A3}$$

where κ is the cavity dissipation rate. This master equation can be solved numerically to obtain the time evolution of the density operator [63].

The polarization resolved reflected output modes, ξ_λ, can be calculated from the cavity mode using input-output theory [64] as $\xi_\lambda(t) = i\mathbf{e}_\lambda^\dagger\mathbf{e}_{\mathrm{in}}\frac{\eta(t)}{\kappa} + \mathbf{e}_\lambda^\dagger\mathbf{A}$ with $\mathbf{e}_\lambda$ the Jones polarization vector describing the polarization mode λ. The H and V polarizations are described by the Jones vectors $\mathbf{e}_H = \frac{1}{\sqrt{2}}(1,1)^{\mathrm{T}}$, $\mathbf{e}_V = \frac{1}{\sqrt{2}}(1,-1)^{\mathrm{T}}$.

APPENDIX B: FIDELITY MEASURES

With the full-time evolution of the cavity-QD density operator, $\rho(t)$, at hand, we can calculate any properties of the system. In particular, we can calculate the fidelity of the composite state consisting of the polarization of scattered light and the internal spin state of the QD. However, this fidelity cannot be evaluated directly from the time-resolved density operator. Care must be taken, because the light polarization must be defined in terms of the reflected light from the cavity, described by the output field operators, $\xi_H(t)$ and $\xi_V(t)$.

First, we consider a single photon scattered on the QD. In general, the two-qubit space spanned by the QD spin and the polarization of the scattered photon can be described by the basis $\mathcal{B}^{(1)} = \{|H\phi_+\rangle, |V\phi_-\rangle, |H\phi_-\rangle, |V\phi_+\rangle\}$, with the superscript (1) signifying that the space spans the polarization of one photon and the QD spin. We denote the true density matrix of the postscattering state of the single-photon–spin system in this basis by $\rho^{(1)}$. We denote by $\chi^{(1)}$ the ideal density operator corresponding to the pure state $|\psi_{\mathrm{pure}}^{(1)}\rangle = \alpha|H\phi_+\rangle + \beta|V\phi_-\rangle$. In the basis $\mathcal{B}^{(1)}$ it takes the form

$$\chi^{(1)} = \begin{pmatrix} |\alpha|^2 & \alpha\beta^* & 0 & 0 \\ \alpha^*\beta & |\beta|^2 & 0 & 0 \\ 0 & 0 & 0 & 0 \\ 0 & 0 & 0 & 0 \end{pmatrix}. \tag{B1}$$

The fidelity between two density operators, ρ_1 and ρ_2, takes the form $\mathcal{F}_{12} = \mathrm{tr}(\rho_1\rho_2)$, if at least one of the density operators is pure. In our case, $\chi^{(1)}$ is pure and we may write the fidelity as

$$\mathcal{F}^{(1)} = |\alpha|^2\rho_{11}^{(1)} + |\beta|^2\rho_{22}^{(1)} + 2\,\mathrm{Re}\{\alpha\beta^*\rho_{21}^{(1)}\}, \tag{B2}$$

which shows that we only need to calculate four matrix elements of $\rho^{(1)}$ to evaluate the fidelity. To evaluate these matrix elements, we define the joint spin-polarization expectation values $\langle S_{P'\lambda'}^{P\lambda}\rangle = \int dt \langle \xi_P^\dagger(t)\xi_{P'}(t)\sigma_{\lambda\lambda'}(t)\rangle/\mathcal{N}^{(1)}$ with $M_{\lambda\lambda'} = |\phi_\lambda\rangle\langle\phi_{\lambda'}|$ the input intensity normalization $\mathcal{N}^{(1)} = \int_{-\infty}^{\infty} dt \xi_{\mathrm{in}}^*(t)\xi_{\mathrm{in}}(t) = \sqrt{\pi/2}\eta_0^2 t_0/\kappa^2$, obtained using $\xi_{\mathrm{in}}(t) = i\eta(t)/\kappa$. This normalization accounts for the fact that we model the incoming photon as a weak coherent pulse. We then find that the $\mathcal{F}^{(1)}$ can be calculated as

$$\mathcal{F}^{(1)} = |\alpha|^2\langle S_{H+}^{H+}\rangle + |\beta|^2|\langle S_{V-}^{H+}\rangle + 2\,\mathrm{Re}[\alpha^*\beta\langle S_{V-}^{V}\rangle].$$

Now we shall consider the scattering of a second photon on the cavity after some time, τ. In Appendix C, we calculate the explicit state, but here we shall simply use the general form for the ideal scattered state

$$|\psi_{\mathrm{pure}}^{(2)}\rangle = \alpha|H_1 H_2\phi_+\rangle + \beta|H_1 V_2\phi_-\rangle$$
$$+ \gamma|V_1 H_2\phi_-\rangle + \delta|V_1 V_2\phi_+\rangle, \tag{B3}$$

with corresponding density operator $\chi^{(2)} = |\psi^{(2)}\rangle\langle\psi^{(2)}|$. Note that the coefficients α and β are not those entering $\chi^{(1)}$. In analogy with the single-photon scattering case, we shall denote the true postscattering density operator by $\rho^{(2)}$. The fidelity becomes

$$\mathcal{F}^{(2)} = |\alpha|^2\langle S_{HH+}^{HH+}\rangle + |\beta|^2\langle S_{HV-}^{HV-}\rangle + |\gamma|^2\langle S_{VH-}^{VH-}\rangle$$
$$+ |\delta|^2\langle S_{VV+}^{VV+}\rangle + 2\,\mathrm{Re}\{\alpha^*\beta\langle S_{HH+}^{HV-}\rangle + \gamma^*\delta\langle S_{VH-}^{VV+}\rangle$$
$$+ e^{ib^x\tau}[\alpha^*\gamma\langle S_{HH+}^{VH-}\rangle + \alpha^*\delta\langle S_{HH+}^{VV+}\rangle$$
$$+ \beta^*\gamma\langle S_{HV-}^{VH-}\rangle + \beta^*\delta\langle S_{HV-}^{VV+}\rangle]\}, \tag{B4}$$

with

$$\langle S_{P'Q'\lambda'}^{PQ\lambda}\rangle = \frac{1}{\mathcal{N}^{(2)}(\tau)}\int dt \langle \xi_P^\dagger(t)\xi_Q^\dagger(t+\tau)$$
$$\times \sigma_{\lambda\lambda'}(t+\tau)\xi_{Q'}(t+\tau)\xi_{P'}(t)\rangle$$

and

$$\mathcal{N}^{(2)}(\tau) = \int_{-\infty}^{\infty} dt\, \xi_{\text{in}}^*(t)\xi_{\text{in}}^*(t+\tau)\xi_{\text{in}}(t+\tau)\xi_{\text{in}}(t)$$

$$= \frac{1}{\kappa^4} \int_{-\infty}^{\infty} dt\, |\eta(t)|^2 |\eta(t+\tau)|^2.$$

Due to the symmetries of the proposed protocol as described in the main text, the fidelity turns out to be independent of the photon separation time, τ.

APPENDIX C: MULTIPHOTON ENTANGLEMENT STRUCTURE

1. Unitary dynamics

The interaction between a string of n photons and the QD can be entirely described by the unitary scattering operator, U, describing the asymptotic composite state resulting from a single-photon scattering event. To find U, we have numerically calculated the postscattering state of four orthogonal initial conditions using the methods described in Appendixes A and B,

$$|H,\omega_0\rangle|\phi_+\rangle \xrightarrow{U} \frac{1}{\sqrt{2}}(|H,\omega_0\rangle|\phi_+\rangle - i|V,\omega_0 + b^H\rangle|\phi_-\rangle),$$

$$|V,\omega_0\rangle|\phi_+\rangle \xrightarrow{U} \frac{1}{\sqrt{2}}(|V,\omega_0\rangle|\phi_+\rangle - i|H,\omega_0 + b^H\rangle|\phi_-\rangle),$$

$$|H,\omega_0\rangle|\phi_-\rangle \xrightarrow{U} \frac{1}{\sqrt{2}}(|H,\omega_0\rangle|\phi_-\rangle + i|V,\omega_0 - b^H\rangle|\phi_+\rangle),$$

$$|V,\omega_0\rangle|\phi_-\rangle \xrightarrow{U} \frac{1}{\sqrt{2}}(|V,\omega_0\rangle|\phi_-\rangle + i|H,\omega_0 - b^H\rangle|\phi_+\rangle).$$

$$(C1)$$

To establish the full unitary operator, we would need to find the evolution of initial conditions with photon frequencies $\omega_0 \pm b$ as well. However, to this end we are only interested in the scattering dynamics of photons resonant with the zero-field QD transition at ω_0. In particular, when restricting the discussion to H-polarized input photons, we only need to know how U works on $|H,\omega_0\rangle|\phi_\pm\rangle$. We then write the total scattered state as

$$|\psi^{(n)}\rangle = \left(\prod_j U_j\right)|H,\omega_0\rangle_1 \cdots |H,\omega_0\rangle_n|\phi_+\rangle, \quad (C2)$$

where U_j acts on the jth photon and the QD. In particular, for two photons, we obtain the state in Eq. (1) of the main text. Generally speaking, the n-photon entangled state has the form $|\psi^{(n)}\rangle = \frac{1}{\sqrt{2}}(|n,+\rangle|\phi_+\rangle + |n,-\rangle|\phi_-\rangle)$. Here, $|n,+\rangle$ contains all superpositions of polarization permutations with an even number of y-polarized photons, where each term in the superposition has a total photonic energy of $n\omega_0$. Similarly, $|n,-\rangle$ contains all terms with an odd number of y-polarized photons and all terms have a photonic energy of $n\omega_0 + b^x$.

2. Entanglement structure of spin-multiphoton state

If we assume that the photon frequency degree of freedom is erased and can be factored out of the remaining state, the gener-

ating scattering transformation, (C1), becomes nonunitary and takes the form $G_j = \frac{1}{\sqrt{2}}(\mathbb{1}_{\text{QD}} \otimes \mathbb{1}_j - Y_{\text{QD}} \otimes X_j)$, with $Y_{\text{QD}} = i(|\phi_-\rangle\langle\phi_+| - |\phi_+\rangle\langle\phi_-|)$ and $X_j = |H\rangle\langle V|_j + |V\rangle\langle H|_j$. Using this form of the scattering operator, we can write down the n-photon–spin entangled state. To do so, we change notation by defining the computational basis for the photon polarization as $|H\rangle_k = |0\rangle_k$, $|V\rangle_k = |1\rangle_k$ and $|\phi_+\rangle = |0\rangle$, $|\phi_-\rangle = |1\rangle$ for the QD spin. The ket subscripts $k = 1,\ldots,n$ shall be used for the photonic qubits, while $k = 0$ denotes the spin qubit. We shall use $i_k \in \{0,1\}$ to denote the value of a qubit in the computational basis, $\mathbf{i} = (i_1,\ldots,i_m)$ denotes an m-bitstring, and $|\mathbf{i}\rangle_{\mathcal{S}}$ the corresponding state with respect to the qubits in the ordered set $\mathcal{S}$. Further, we shall neglect normalization factors for ease of notation. The n-photon scattered state can then be written as

$$|\psi^{(n)}\rangle = \prod_j G_j |0,\ldots,0\rangle_{\{0,\ldots,n\}}$$

$$= |0\rangle_0 \sum_{\mathbf{i} \in S_e(n)} |\mathbf{i}\rangle_{\{1,\ldots,n\}} - i|1\rangle_0 \sum_{\mathbf{i} \in S_o(n)} |\mathbf{i}\rangle_{\{1,\ldots,n\}}, \quad (C3)$$

with $S_e(n) = \{i_1,\ldots,i_n | \sum_k i_k = 2m, m \in \mathbb{N}\}$ and $S_o(n) = \{i_1,\ldots,i_n | \sum_k i_k = 2m + 1, m \in \mathbb{N}\}$. By singling out the kth, lth, and mth photonic qubits from the sums, we can rewrite this state as

$$|\psi^{(n)}\rangle = |c'_+\rangle_{klm}|R_+\rangle + |c'_-\rangle_{klm}|R_-\rangle, \quad (C4)$$

with the k,l,m-qubit states $|c'_+\rangle = |000\rangle + |110\rangle + |011\rangle + |101\rangle$, $|c'_-\rangle = |001\rangle + |111\rangle + |010\rangle + |100\rangle$ and the residual qubit states

$$|R_+\rangle = |0\rangle_0 \sum_{\mathbf{i} \in S_e(n-3)} |\mathbf{i}\rangle_{\{1,\ldots,n\}\setminus\{k,l,m\}}$$

$$- i|1\rangle_0 \sum_{\mathbf{i} \in S_o(n-3)} |\mathbf{i}\rangle_{\{1,\ldots,n\}\setminus\{k,l,m\}},$$

$$|R_-\rangle = |0\rangle_0 \sum_{\mathbf{i} \in S_o(n-3)} |\mathbf{i}\rangle_{\{1,\ldots,n\}\setminus\{k,l,m\}}$$

$$- i|1\rangle_0 \sum_{\mathbf{i} \in S_e(n-3)} |\mathbf{i}\rangle_{\{1,\ldots,n\}\setminus\{k,l,m\}}. \quad (C5)$$

The states $|c'_\pm\rangle_{klm}$ are local unitary equivalent to three-qubit linear cluster states, which are local unitary equivalent to three-photon GHZ states [65]. This is seen by applying the Hadamard transformation, $\mathcal{H} = |0\rangle\langle0| + |1\rangle\langle0| + |0\rangle\langle1| - |1\rangle\langle1|$ to the lth photon, $\mathcal{H}_l|c'_\pm\rangle_{\{klm\}} = |c_\pm\rangle_{\{klm\}}$, where $|c_\pm\rangle$ are the two orthogonal cluster states $|000\rangle \pm |111\rangle + |100\rangle \mp |110\rangle + |001\rangle \mp |011\rangle + |101\rangle \pm |111\rangle$. From this form, we can easily calculate all single-qubit reduced density operators, which all take the form $\rho_k = \mathbb{1}$. Furthermore, we can calculate the two-qubit reduced density operators, which for two photonic qubits, kl, take the form $\rho_{kl} = |\mathcal{B}_1\rangle\langle\mathcal{B}_1| + |\mathcal{B}_2\rangle\langle\mathcal{B}_2|$ with the two Bell states $|\mathcal{B}_1\rangle = |00\rangle + |11\rangle$, $|\mathcal{B}_2\rangle = |01\rangle + |10\rangle$. Two-qubit reduced density operators involving the spin qubit take the similar form $\rho_{0k} = |\mathcal{B}'_1\rangle\langle\mathcal{B}'_1| + |\mathcal{B}'_2\rangle\langle\mathcal{B}'_2|$ with the rotated Bell states $|\mathcal{B}'_1\rangle = |00\rangle - i|11\rangle$, $|\mathcal{B}'_2\rangle = |01\rangle - i|10\rangle$. From these reduced density operators, we can show that the generated state is not local unitary equivalent to a linear cluster state for more than three qubits. This is due to the necessary condition for local unitary equivalence that all reduced density

operators must also be local unitary equivalent [66]. Since for a linear cluster state with more than three qubits there exist indices kl such that $\rho_{kl} = \mathbb{1}$, the two states cannot be local unitary equivalent.

However, from (C4), we can infer that performing local projective measurements on *any* $n - 3$ photons and the spin in the computational basis leaves the remaining three photons in an entangled state that is local unitary equivalent to a three-qubit GHZ or linear cluster state. This also holds in the particular case where there are only three photons in the scattered state, and a projective measurement is performed on the spin. A similar series of local measurements on $n - 2$ photons and the spin leaves the remaining two photons in a Bell state, which is maximally entangled. Since these properties do not depend on the indices of the photonic qubits, we infer that the localizable entanglement is maximal and the entanglement length is infinite [67].

APPENDIX D: ANALYSIS OF PROTOCOL B

A protocol very similar to the one proposed in the main text has been used for generation of entanglement between a single photon and a QD [43,50,51]. Here, the QD is initialized in the $|\phi_+\rangle$ ground state and excited to $\frac{1}{\sqrt{2}}(|\Uparrow\rangle + |\Downarrow\rangle)$ by an H-polarized π pulse resonant with the transition $|\phi_+\rangle \leftrightarrow \frac{1}{\sqrt{2}}(|\Uparrow\rangle + |\Downarrow\rangle)$ at $\omega_0 - b^x/2$. As this state decays, a photon is emitted, which is entangled with the spin of the QD,

$$|\psi^{(1)}\rangle = c_H|H,\omega_0 - b^x/2\rangle_1|\phi_+\rangle + c_V|V,\omega_0 + b^x/2\rangle_1|\phi_-\rangle,$$
$$(D1)$$

with $|c_i|^2 = 1/2$. This state is protected against dephasing, because both terms in the superposition have the same total energy of ω_0. To add a second photon to the state, the QD is excited again. This time, we have to use a two-color π pulse, because the QD is in a superposition of the two ground states. Immediately after the excitation, the system is in the state

$$c_H|H, -b^x/2\rangle_1 \frac{|\Uparrow\rangle + |\Downarrow\rangle}{\sqrt{2}} + c_V|V, +b^x/2\rangle_1 \frac{|\Uparrow\rangle - |\Downarrow\rangle}{\sqrt{2}},$$
$$(D2)$$

where we have transformed to a frame rotating with ω_0. As the QD decays, the state becomes

$$|\psi^{(2)}\rangle = c_{HH}|H,-b^x/2\rangle_1|H,-b^x/2\rangle_2|\phi_+\rangle$$
$$+ c_{HV}|H,-b^x/2\rangle_1|V,+b^x/2\rangle_2|\phi_-\rangle$$
$$+ c_{VH}|V,+b^x/2\rangle_1|H,+b^x/2\rangle_2|\phi_-\rangle$$
$$+ c_{VV}|V,+b^x/2\rangle_1|V,-b^x/2\rangle_2|\phi_+\rangle, \quad (D3)$$

with $|c_{\alpha\beta}|^2 = 1/4$ Here, the two first terms have an energy of $-b^x/2$, whereas the two last terms have an energy of $+b^x/2$. In the time until the next excitation event, τ, the state will evolve

freely. Recalling that $b^x = b^x_{\text{ext}} + b^x_{\text{N}}$, the time evolution is

$$|\psi^{(2)},\tau\rangle = e^{+i(b^x_{\text{ext}}+b^x_{\text{N}})\tau/2}[c_{HH}|H, -b^x/2\rangle_1|H, -b^x/2\rangle_2|\phi_+\rangle$$
$$+ c_{HV}|H, -b^x/2\rangle_1|V, +b^x/2\rangle_2|\phi_-\rangle]$$
$$+ e^{-i(b^x_{\text{ext}}+b^x_{\text{N}})\tau/2}[c_{VH}|V,+b^x/2\rangle_1|H,+b^x/2\rangle_2|\phi_-\rangle$$
$$+ c_{VV}|V, +b^x/2\rangle_1|V, -b^x/2\rangle_2|\phi_+\rangle]. \quad (D4)$$

The fidelity with respect to $|\psi^{(2)}\rangle$ is $|\langle\psi^{(2)}|\psi^{(2)},\tau\rangle|^2 = \frac{1}{2}\{1 + \cos[(b^x_{\text{ext}} + b^x_{\text{N}})\tau]\}$. On performing an ensemble average over the weight distribution of the Overhauser field, the fidelity becomes $\mathcal{F} = \frac{1}{2}\int_{-\infty}^{\infty} db^x_{\text{N}} w(b^x_{\text{N}}; \delta_b)\{1 + \cos[(b^x_{\text{ext}} + b^x_{\text{N}})\tau]\} = \frac{1}{2}\{1 + e^{-(\tau/T_2^*)^2}\cos(b^x_{\text{ext}}\tau)\}$, with $T_2^* = \sqrt{2}/(g_e\mu_B\Delta_B)$. Such dephasing processes will take place between all of the following excitation events. The time between excitations is limited by the lifetime of the QD, and if we assume that this is much shorter than the coherence time, T_2^*, we may neglect dephasing between excitations for a few photons. However, after spin projection, the photonic state will be subject to dephasing of the same nature. Measuring the spin in the basis $\{\phi_+,\phi_-\}$ leaves the two emitted photons in either of the two states:

$$|\psi_+^{(2)}\rangle = \sqrt{2}\,\langle\phi_+|\psi^{(2)}\rangle$$
$$= \sqrt{2}[c_{HH}|H, -b^x/2\rangle_1|H, -b^x/2\rangle_2$$
$$+ c_{VV}|V, +b^x/2\rangle_1|V, -b^x/2\rangle_2],$$
$$|\psi_-^{(2)}\rangle = \sqrt{2}\,\langle\phi_-|\psi^{(2)}\rangle$$
$$= \sqrt{2}[c_{HV}|H, -b^x/2\rangle_1|V, +b^x/2\rangle_2$$
$$+ c_{VH}|V, +b^x/2\rangle_1|H, +b^x/2\rangle_2]. \quad (D5)$$

After the projective measurement, the states evolve as

$$|\psi_+^{(2)},t\rangle = \sqrt{2}\,\langle\phi_+|\psi^{(2)}\rangle$$
$$= \sqrt{2}[c_{HH}e^{+i(b^x_{\text{ext}}+b^x_{\text{N}})t}|H, -b^x/2\rangle_1|H, -b^x/2\rangle_2$$
$$+ c_{VV}|V, +b^x/2\rangle_1|V, -b^x/2\rangle_2],$$
$$|\psi_-^{(2)},t\rangle = \sqrt{2}\,\langle\phi_-|\psi^{(2)}\rangle = \sqrt{2}[c_{HV}|H,-b^x/2\rangle_1|V,+b^x/2\rangle_2$$
$$+ c_{VH}e^{-i(b^x_{\text{ext}}+b^x_{\text{N}})t}|V, +b^x/2\rangle_1|H, +b^x/2\rangle_2]. \quad (D6)$$

The fidelity of these states with respect to the $|\psi_\pm^{(2)}\rangle$ is $f_\pm = |\langle\psi_\pm^{(2)}|\psi_\pm^{(2)},t\rangle|^2$. Since the outcome of the projective spin measurement is $|\phi_+\rangle$ and $|\phi_-\rangle$ with equal probability, the average fidelity is $\frac{1}{2}(f_+ + f_-)$. When performing an ensemble average over the Overhauser weight distribution, the resulting fidelity is $\mathcal{F}^{(2)} = \frac{1}{2}\int_{-\infty}^{\infty} db^x_{\text{N}} w(b^x_{\text{N}}; \delta_b)(f_+ + f_-) = \frac{1}{2}\{1 + e^{-(t/T_2^*)^2}\cos(b^x_{\text{ext}}t)\}$. In conclusion, the fidelity of the photonic state after spin projection decays with a time scale of T_2^*. This calculation can straightforwardly be extended to cover the spin-projected three-photon state, yielding a fidelity of $\mathcal{F}^{(3)} = \frac{1}{8}\{3 + 4e^{-(t/T_2^*)^2}\cos(b^x_{\text{ext}}) + e^{-(2t/T_2^*)^2}\cos(2b^x_{\text{ext}})\}$.

[1] T. D. Ladd, F. Jelezko, R. Laflamme, Y. Nakamura, C. Monroe, and J. L. O'Brien, Nature (London) **464**, 45 (2010).

[2] M. A. Nielsen and I. Chuang, *Quantum Computation and Quantum Information* (Cambridge University Press, Cambridge, UK, 2010).

[3] N. Gisin, G. Ribordy, W. Tittel, and H. Zbinden, Rev. Mod. Phys. **74**, 145 (2002).

[4] A. K. Ekert, Phys. Rev. Lett. **67**, 661 (1991).

[5] C. H. Bennett, G. Brassard, C. Crépeau, R. Jozsa, A. Peres, and W. K. Wootters, Phys. Rev. Lett. **70**, 1895 (1993).

[6] T.-J. Wang, S.-Y. Song, and G. L. Long, Phys. Rev. A **85**, 062311 (2012).

[7] R. Raussendorf and H. J. Briegel, Phys. Rev. Lett. **86**, 5188 (2001).

[8] R. Raussendorf, D. E. Browne, and H. J. Briegel, Phys. Rev. A **68**, 022312 (2003).

[9] H. J. Briegel, D. E. Browne, W. Dür, R. Raussendorf, and M. Van den Nest, Nat. Phys. **5**, 19 (2009).

[10] P. Kok, W. J. Munro, K. Nemoto, T. C. Ralph, J. P. Dowling, and G. J. Milburn, Rev. Mod. Phys. **79**, 135 (2007).

[11] S. Yokoyama, R. Ukai, S. C. Armstrong, C. Sornphiphat-phong, T. Kaji, S. Suzuki, J.-i. Yoshikawa, H. Yonezawa, N. C. Menicucci, and A. Furusawa, Nat. Photon. **7**, 982 (2013).

[12] P. G. Kwiat, E. Waks, A. G. White, I. Appelbaum, and P. H. Eberhard, Phys. Rev. A **60**, R773 (1999).

[13] E. Togan, Y. Chu, A. S. Trifonov, L. Jiang, J. Maze, L. Childress, M. V. G. Dutt, A. S. Sorensen, P. R. Hemmer, A. S. Zibrov, and M. D. Lukin, Nature (London) **466**, 730 (2010).

[14] I. Schwartz, D. Cogan, E. R. Schmidgall, Y. Don, L. Gantz, O. Kenneth, N. H. Lindner, and D. Gershoni, Science **354**, 434 (2016).

[15] J. Claudon, J. Bleuse, N. S. Malik, M. Bazin, P. Jaffrennou, N. Gregersen, C. Sauvan, P. Lalanne, and J.-M. Gérard, Nat. Photon. **4**, 174 (2010).

[16] O. Gazzano, S. M. de Vasconcellos, C. Arnold, A. Nowak, E. Galopin, I. Sagnes, L. Lanco, A. Lemaître, and P. Senellart, Nat. Commun. **4**, 1425 (2013).

[17] N. Somaschi, V. Giesz, L. De Santis, J. Loredo, M. Almeida, G. Hornecker, S. Portalupi, T. Grange, C. Anton, J. Demory *et al.*, Nat. Photon. **10**, 340 (2016).

[18] Y.-M. He, Y. He, Y.-J. Wei, D. Wu, M. Atatüre, C. Schneider, S. Höfling, M. Kamp, C.-Y. Lu, and J.-W. Pan, Nat. Nanotechnol. **8**, 213 (2013).

[19] J. Iles-Smith, D. P. S. McCutcheon, A. Nazir, and J. Mørk, Nat. Photon. **11**, 521 (2017).

[20] M. Arcari, I. Söllner, A. Javadi, S. L. Hansen, S. Mahmoodian, J. Liu, H. Thyrrestrup, E. H. Lee, J. D. Song, S. Stobbe *et al.*, Phys. Rev. Lett. **113**, 093603 (2014).

[21] M. Bayer, G. Ortner, O. Stern, A. Kuther, A. A. Gorbunov, A. Forchel, P. Hawrylak, S. Fafard, K. Hinzer, T. L. Reinecke *et al.*, Phys. Rev. B **65**, 195315 (2002).

[22] M. Atatüre, J. Dreiser, A. Badolato, A. Högele, K. Karrai, and A. Imamoğlu, Science **312**, 551 (2006).

[23] X. Xu, Y. Wu, B. Sun, Q. Huang, J. Cheng, D. G. Steel, A. S. Bracker, D. Gammon, C. Emary, and L. J. Sham, Phys. Rev. Lett. **99**, 097401 (2007).

[24] J. Berezovsky, M. H. Mikkelsen, N. G. Stoltz, L. A. Coldren, and D. D. Awschalom, Science **320**, 349 (2008).

[25] D. Press, T. D. Ladd, B. Zhang, and Y. Yamamoto, Nature (London) **456**, 218 (2008).

[26] E. D. Kim, K. Truex, X. Xu, B. Sun, D. G. Steel, A. S. Bracker, D. Gammon, and L. J. Sham, Phys. Rev. Lett. **104**, 167401 (2010).

[27] A. Delteil, W. B. Gao, P. Fallahi, J. Miguel-Sanchez, and A. Imamoğlu, Phys. Rev. Lett. **112**, 116802 (2014).

[28] S. G. Carter, T. M. Sweeney, M. Kim, C. S. Kim, D. Solenov, S. E. Economou, T. L. Reinecke, L. Yang, A. S. Bracker, and D. Gammon, Nat. Photon. **7**, 329 (2013).

[29] S. Sun and E. Waks, Phys. Rev. A **94**, 012307 (2016).

[30] W. B. Gao, A. Imamoğlu, H. Bernien, and R. Hanson, Nat. Photon. **9**, 363 (2015).

[31] C. Y. Hu, W. J. Munro, and J. G. Rarity, Phys. Rev. B **78**, 125318 (2008).

[32] A. Pineiro-Orioli, D. P. S. McCutcheon, and T. Rudolph, Phys. Rev. B **88**, 035315 (2013).

[33] N. H. Lindner and T. Rudolph, Phys. Rev. Lett. **103**, 113602 (2009).

[34] S. E. Economou, N. Lindner, and T. Rudolph, Phys. Rev. Lett. **105**, 093601 (2010).

[35] D. Buterakos, E. Barnes, and S. E. Economou, Phys. Rev. X **7**, 041023 (2017).

[36] D. P. S. McCutcheon, N. H. Lindner, and T. Rudolph, Phys. Rev. Lett. **113**, 260503 (2014).

[37] I. A. Merkulov, A. L. Efros, and M. Rosen, Phys. Rev. B **65**, 205309 (2002).

[38] D. Press, K. De Greve, P. L. McMahon, T. D. Ladd, B. Friess, C. Schneider, M. Kamp, S. Höfling, A. Forchel, and Y. Yamamoto, Nat. Photon. **4**, 367 (2010).

[39] B. Urbaszek, X. Marie, T. Amand, O. Krebs, P. Voisin, P. Maletinsky, A. Högele, and A. Imamoglu, Rev. Mod. Phys. **85**, 79 (2013).

[40] A. V. Kuhlmann, J. Houel, A. Ludwig, L. Greuter, D. Reuter, A. D. Wieck, M. Poggio, and R. J. Warburton, Nat. Phys. **9**, 570 (2013).

[41] M. N. Leuenberger and M. Erementchouk, in *SPIE Sensing Technology + Applications* (International Society for Optics and Photonics, Baltimore, Maryland, 2014), pp. 91230I–91230I.

[42] T. L. Vu, S. S. Ge, and C. C. Hang, Phys. Rev. A **85**, 012332 (2012).

[43] W. B. Gao, P. Fallahi, E. Togan, J. Miguel-Sánchez, and A. Imamoğlu, Nature (London) **491**, 426 (2012).

[44] G. Éthier-Majcher, D. Gangloff, R. Stockill, E. Clarke, M. Hugues, C. Le Gall, and M. Atatüre, Phys. Rev. Lett. **119**, 130503 (2017).

[45] E. A. Chekhovich, M. N. Makhonin, A. I. Tartakovskii, A. Yacoby, H. Bluhm, K. C. Nowack, and L. M. K. Vandersypen, Nat. Mater. **12**, 494 (2013).

[46] P. Maletinsky, A. Badolato, and A. Imamoğlu, Phys. Rev. Lett. **99**, 056804 (2007).

[47] A. S. Bracker, E. A. Stinaff, D. Gammon, M. E. Ware, J. G. Tischler, A. Shabaev, A. L. Efros, D. Park, D. Gershoni, V. L. Korenev *et al.*, Phys. Rev. Lett. **94**, 047402 (2005).

[48] A. Imamoğlu, E. Knill, L. Tian, and P. Zoller, Phys. Rev. Lett. **91**, 017402 (2003).

[49] C. W. Lai, P. Maletinsky, A. Badolato, and A. Imamoğlu, Phys. Rev. Lett. **96**, 167403 (2006).

[50] J. R. Schaibley, A. P. Burgers, G. A. McCracken, L.-M. Duan, P. R. Berman, D. G. Steel, A. S. Bracker, D. Gammon, and L. J. Sham, Phys. Rev. Lett. **110**, 167401 (2013).

[51] K. De Greve, L. Yu, P. L. McMahon, J. S. Pelc, C. M. Natarajan, N. Y. Kim, E. Abe, S. Maier, C. Schneider, M. Kamp *et al.*, Nature (London) **491**, 421 (2012).

[52] M. Gimeno-Segovia, P. Shadbolt, D. E. Browne, and T. Rudolph, Phys. Rev. Lett. **115**, 020502 (2015).

[53] Alternatively, the polarization information can be erased in order to achieve qutrit color entanglement. However, we shall not discuss this possibility further in this paper.

[54] Ł. Cywiński, W. M. Witzel, and S. DasSarma, Phys. Rev. Lett. **102**, 057601 (2009).

[55] A. Reigue, J. Iles-Smith, F. Lux, L. Monniello, M. Bernard, F. Margaillan, A. Lemaitre, A. Martinez, D. P. S. McCutcheon, J. Mørk *et al.*, Phys. Rev. Lett. **118**, 233602 (2017).

[56] We restrict our analysis to the ideal case, where no hole mixing is present.

[57] J. R. Johansson, P. D. Nation, and F. Nori, Comput. Phys. Commun. **184**, 1234 (2013).

[58] We note that the frequency information is erased automatically in our computational model by projecting the photonic state onto a broad cavity quasimode. Thus we calculate the fidelity in the limit of a perfect frequency erasure.

[59] J. R. Schaibley and P. R. Berman, J. Phys. B **45**, 124020 (2012).

[60] S. E. Economou, R.-B. Liu, L. J. Sham, and D. G. Steel, Phys. Rev. B **71**, 195327 (2005).

[61] J. Fischer, W. A. Coish, D. V. Bulaev, and D. Loss, Phys. Rev. B **78**, 155329 (2008).

[62] H. J. Carmichael, *Statistical Methods in Quantum Optics 1: Master Equations and Fokker-Planck Equations* (Springer Science & Business Media, New York, 2009).

[63] J. R. Johansson, P. D. Nation, and F. Nori, Comput. Phys. Commun. **183**, 1760 (2012).

[64] D. A. Steck, http://atomoptics-nas.uoregon.edu/~dsteck/teaching/quantum-optics/quantum-optics-notes.pdf

[65] D. M. Greenberger, M. A. Horne, and A. Zeilinger, *Bell's Theorem, Quantum Theory and Conceptions of the Universe* (Springer, New York, 1989), pp. 69–72.

[66] B. Kraus, Phys. Rev. Lett. **104**, 020504 (2010).

[67] M. Popp, F. Verstraete, M. A. Martín-Delgado, and J. I. Cirac, Phys. Rev. A **71**, 042306 (2005).